

# A renormalization approach to quantum thermal annealing

Yong-Han Lee<sup>a</sup> and B. J. Berne

Department of Chemistry and Center for Biomolecular Simulation, Columbia University,  
3000 Broadway, New York, New York 10027  
yh1@chem.columbia.edu, berne@chem.columbia.edu

Received 5 August 2000, accepted 16 August 2000

**Abstract.** The details of an efficient global optimization approach, quantum thermal annealing with renormalization (QTAR) (Y. H. Lee and B. J. Berne, *J. Phys. Chem. A*, in press (2000)) are presented in this paper. This method is based on the application of the Migdal-Kadanoff method for decimating Trotter time slices in the staging and primitive algorithms for sampling path integrals using Monte Carlo methods. In a nutshell, one starts in a strong quantum regime where the number of Trotter beads representing each quantum particle and the value of Planck’s constant are large, thereby allowing for efficient tunneling through the barriers of a rough energy landscape typical in the folding of proteins, and anneals the system methodically to the classical limit where the values of the aforementioned quantities are 1 and 0, respectively. Global optimization of the system is achieved through the iterative use of such quantum-to-classical annealing cycles. The QTAR algorithm applied to a highly frustrated BLN model protein with 46 residues more efficiently locates the global energy minimum than established methods like simulated annealing.

**Keywords:** global optimization, renormalization, path integral methods, proteins

**PACS:** 05.10.Cc, 05.10.-a, 31.15.Kb

## 1 Introduction

In this paper, we outline an efficient global optimization algorithm, quantum thermal annealing with renormalization (QTAR), that is able to locate global energy minima in complex systems with rough energy landscapes. This method finds the global minimum of a system by annealing it from the quantum regime back to the classical realm. In a previous publication [1], we have shown that quantization of a system moving on a very rough energy landscape softens its potential, thus allowing for faster convergence to its classical ground state upon annealing. The amount of “quantumness” of the system was controlled and annealed essentially through Planck’s “constant”  $\hbar$ . In fact, one can go further with quantum thermal annealing by enhancing the quantization of the system to a much higher degree. In a path integral Monte Carlo (PIMC) approach, this means the use of a large Trotter number  $P$  to represent the system in the beginning. This allows for very effective tunneling events during the course of a simulation run. This increase in the number of degrees of freedom is tamed

---

<sup>a</sup> In partial fulfillment of the Ph.D. in the Department of Physics, Columbia University.

by systematically reducing the number of Trotter beads during annealing, through the use of a renormalization approach [2]. In addition to cost saving, this method also allows the isomorphic classical system to sample a hierarchy of energy and length scales in its search for the global minimum. We note that many useful global optimization algorithms [3–19] are available. However, very rugged or frustrated energy landscapes might present difficulties for various methods in practice. QTAR is very effective in dealing with such problems. The main aim of the current paper is to present the details of the renormalization approach used to manage the sampling of the path integrals in QTAR. The algorithm is then tested on a well known frustrated system, a 46-residue BLN model protein of Honeycutt and Thirumalai [20–22], with very encouraging results.

This article is organized as follows. In Sec. 2, we present a brief overview of the underlying physical and computational foundations of QTAR. In Sec. 3, we study in detail the renormalization methodology used in our approach, including the derivation of relevant renormalization transformations of the Hamiltonians used in our scheme. Sec. 4 describes the BLN protein model and the QTAR annealing schedule employed to locate the global minimum of the frustrated 46-mer. In addition, we summarize the results of a comparative study of the global optimization of the aforementioned protein using QTAR and simulated annealing. The conclusions are presented in Sec. 5.

## 2 Method

The quantum canonical partition function in Feynman’s formulation of quantum statistical mechanics is written in terms of a path integral [23]. The path integral can be discretized in different ways for computational purposes. Two such discrete expressions are results of the primitive approximation [24–27] and staging transformation [28, 29]. For a system of size  $N$  in 3 dimensions, the partition function with the primitive Hamiltonian is given by

$$Q_P^{\text{prim}}(\beta) = \left( \frac{Pm}{2\pi\beta\hbar^2} \right)^{3NP/2} \int d\mathbf{r}_{1,1} \cdots d\mathbf{r}_{i,t} \cdots d\mathbf{r}_{N,P} \quad (1)$$

$$\times \exp \left[ -\beta \left( \sum_{i=1}^N \sum_{t=1}^P \frac{m\omega_P^2}{2} |\mathbf{r}_{i,t} - \mathbf{r}_{i,t+1}|^2 + \frac{1}{P} \sum_{t=1}^P V_{\text{cl}}(\{\mathbf{r}_i\}; t) \right) \right],$$

where the Trotter number  $P$  is an integer that denotes the number of “time” slices used in the discretization, and  $\omega_P \equiv (\beta\hbar)^{-1}\sqrt{P}$ . The 3-vector position of the Trotter bead of the  $i$ -th particle in the  $t$ -th time slice is given by  $\mathbf{r}_{i,t}$ , while the total classical potential energy evaluated at time slice  $t$  is represented by  $V_{\text{cl}}(\{\mathbf{r}_i\}; t)$ .  $P$  is a measure of the “quantumness” of a system: accurate treatment of a highly quantum system requires a large value for  $P$ , while a purely classical system has  $P = 1$ . In fact, the equilibrium properties of a strongly quantum system, where  $P$  is large, can be sampled more efficiently with the staging Hamiltonian. The corresponding partition function

is [29]

$$\begin{aligned}
 Q_P^{\text{stag}}(\beta) = & \left\{ \frac{\beta m \omega_j^2}{2\pi} \prod_{k=2}^j \left( \frac{\beta m_k \omega_P^2}{2\pi} \right) \right\}^{3Nn/2} \int d\mathbf{u}_{1,1} \cdots d\mathbf{u}_{i,t} \cdots d\mathbf{u}_{N,P} \\
 & \times \exp \left[ -\beta \left( \sum_{i=1}^N \sum_{s=0}^{n-1} \frac{m \omega_j^2}{2} |\mathbf{u}_{i,sj+1} - \mathbf{u}_{i,(s+1)j+1}|^2 \right. \right. \\
 & \left. \left. + \sum_{i=1}^N \sum_{s=0}^{n-1} \sum_{k=2}^j \frac{m_k \omega_P^2}{2} \mathbf{u}_{i,sj+k}^2 + \frac{1}{P} \sum_{t=1}^P V_{\text{cl}}(\{\mathbf{r}_i(\mathbf{u})\}; t) \right) \right], \quad (2)
 \end{aligned}$$

with  $nj = P$ , where  $n$  and  $j$  are the number of end-point and staging Trotter beads, respectively. The staging coordinates are  $\mathbf{u}_{i,t}$ , with  $m_k = mk/(k-1)$  and  $\omega_j \equiv (\beta\hbar)^{-1} \sqrt{P/j}$ .

The other quantity in our formalism that determines the “quantumness” of a system is Planck’s “constant”  $\hbar$ . We use it as an adjustable *parameter*: a large value for  $\hbar$  represents a strong quantum regime, while  $\hbar = 0$  gives us the classical limit. For the present QTAR method, quantum thermal annealing is achieved by methodically reducing both  $P$  and  $\hbar$ . In each quantum-to-classical cycle, we wish to systematically remove half of the total number of Trotter time slices of the primitive or staging Hamiltonians in stages until we reach  $P = 1$  (classical regime):

$$P_0 \longrightarrow \frac{P_0}{2^1} \longrightarrow \frac{P_0}{2^2} \longrightarrow \frac{P_0}{2^3} \longrightarrow \cdots \longrightarrow 2 \longrightarrow 1, \quad (3)$$

where  $P_0 = 2^\alpha$  ( $\alpha \geq 1$ ) is the initial number of Trotter time slices used. During this process,  $\hbar$  is annealed from  $\hbar_0$  to 0, and temperature  $T$  from  $T_0$  to 0 as well. The reduction in  $P$  is accomplished through the use of a renormalization approach for both Hamiltonians. The number of Trotter beads  $P$  is held constant between renormalizations, and the system is allowed to explore configuration space via PIMC moves during this time. In the next section, we take a more detailed look at the renormalization aspect of the QTAR method.

### 3 Renormalization in QTAR

To achieve the reduction in the number of degrees of freedom as stipulated by (3), one has a choice among different types of renormalization schemes. The Migdal-Kadanoff (MK) approach [30–32] is chosen here because it provides a simple way to incorporate renormalization in QTAR. First, MK bond moving operations are performed whereby all bonds representing  $V_{\text{cl}}(\{\mathbf{r}_i\}; t)$  with odd-numbered Trotter time slices are moved to their *adjacent* even-numbered sites (the designation of odd and even is arbitrary). As a result, instead of having  $V_{\text{cl}}(\{\mathbf{r}_i\}; t = a+1)$  at a particular time slice  $t = a+1$  (which is even), we now have 2 sets of bonds  $V_{\text{cl}}(\{\mathbf{r}_i\}; t = a+1) + V_{\text{cl}}(\{\mathbf{r}_i\}; t = a)$  at  $t = a+1$ . The MK transformation was originally devised for lattice systems like the Ising model. However, the BLN 46-mer and other chemical and biological molecules which we are interested in are off-lattice objects. Consequently, these bond-moving operations do

not in general result in bonds that fall exactly on top of their targets. Fortunately, since the configurations corresponding to time slices  $t = a + 1$  and  $t = a$  are adjacent, they are expected to be quite comparable to each other in terms of configuration and thus energy. Thus, we take

$$\begin{aligned} V_{\text{cl}}(\{\mathbf{r}_i\}; t = a + 1) + V_{\text{cl}}(\{\mathbf{r}_i\}; t = a) \\ \approx V_{\text{cl}}(\{\mathbf{r}_i\}; t = a + 1) + V_{\text{cl}}(\{\mathbf{r}_i\}; t = a + 1) \\ = 2V_{\text{cl}}(\{\mathbf{r}_i\}; t = a + 1). \end{aligned} \quad (4)$$

If one wishes to move more than one set of bonds (say  $p$  of them) instead of just the nearest-neighbor set, the approximation above is expected to be less valid since it is not likely that all  $p$  adjacent configurations would be similar to one another. Other renormalization schemes such as those that involve potential averaging might be more suitable for such a case. However, in addition to the possibility of being more tedious to implement computationally, these would also add extra computational costs to the scheme. Hence for quantum thermal annealing purposes, the MK approach is more appropriate and useful. After performing the MK bond-moving operations, all the odd-numbered Trotter beads can be integrated (decimated) out. This is because they are now free from the external potential  $V_{\text{cl}}(\{\mathbf{r}_i\}; t)$ , and are only coupled to adjacent even-numbered beads through the usual harmonic potential. The outcome is rather simple. For the primitive Hamiltonian, the functional form remains the same as in Eq. (1), but with  $P$  replaced by  $P' = P/2$ . The MK renormalization of the staging Hamiltonian, while more involved, gives an analogous result. This will be investigated in the next subsection.

### 3.1 Migdal-Kadanoff renormalization of the staging Hamiltonian

We start by performing the Migdal-Kadanoff bond-moving operation on alternate staging beads of the quantum chain of each particle. Upon doing this, we end up with the following for the partition function of the staging Hamiltonian:

$$\begin{aligned} Q_P^{\text{stag}}(\beta) = & \left\{ \frac{\beta m \omega_j^2}{2\pi} \prod_{k=2}^j \left( \frac{\beta m_k \omega_P^2}{2\pi} \right) \right\}^{3Nn/2} \int d\mathbf{u}_{1,1} \cdots d\mathbf{u}_{i,t} \cdots d\mathbf{u}_{N,P} \\ & \times \exp \left[ -\beta \left( \sum_{i=1}^N \sum_{s=0}^{n-1} \frac{m \omega_j^2}{2} |\mathbf{u}_{i,sj+1} - \mathbf{u}_{i,(s+1)j+1}|^2 \right. \right. \\ & \left. \left. + \sum_{i=1}^N \sum_{s=0}^{n-1} \sum_{k=2}^j \frac{m_k \omega_P^2}{2} \mathbf{u}_{i,sj+k}^2 + \frac{1}{P} \sum_{\substack{t=1 \\ t \text{ odd only}}}^P 2V_{\text{cl}}(\{\mathbf{r}_i(\mathbf{u})\}; t) \right) \right]. \end{aligned} \quad (5)$$

Hence, all the even-numbered Trotter beads are now free from  $V_{\text{cl}}(\{\mathbf{r}_i(\mathbf{u})\}; t)$ , the external potential, and are only subjected to the influence of the staging potential.

These beads can readily be decimated out to give:

$$\begin{aligned}
 Q_{P/2}^{\text{stag}}(\beta) &= \left\{ \frac{\beta m \omega_j^2}{2\pi} \prod_{k=2}^j \left( \frac{\beta \alpha_k}{\pi} \right) \prod_{\substack{k=2 \\ k \text{ even only}}}^j \left( \frac{\pi}{\beta \alpha_k} \right) \right\}^{3Nn/2} \int \overbrace{d\mathbf{u}_{1,1} \cdots d\mathbf{u}_{i,t} \cdots d\mathbf{u}_{N,P}}^{t \text{ odd only}} \\
 &\times \exp \left[ -\beta \left( \sum_{i=1}^N \sum_{s=0}^{n-1} \frac{m \omega_j^2}{2} |\mathbf{u}_{i,sj+1} - \mathbf{u}_{i,(s+1)j+1}|^2 \right. \right. \\
 &\quad \left. \left. + \sum_{i=1}^N \sum_{s=0}^{n-1} \sum_{\substack{k=2 \\ k \text{ odd only}}}^j \alpha_k \mathbf{u}_{i,sj+k}^2 + \frac{2}{P} \sum_{\substack{t=1 \\ t \text{ odd only}}}^P V_{\text{cl}}(\{\mathbf{r}_i(\mathbf{u})\}; t) \right) \right], \quad (6)
 \end{aligned}$$

where  $\alpha_k \equiv m_k \omega_P^2 / 2$ .

Since  $P/2$  Trotter beads have been integrated out, we change the subscript of the partition function from  $P$  in Eq. (5) to  $P/2$  in Eq. (6). At this point, we have  $n$  end-point beads and  $j/2$  staging beads to give a total of  $P/2$  beads, i.e.  $nj/2 = P/2$ . In what follows, we show how one could recover the exact form of the staging Hamiltonian from  $Q_{P/2}^{\text{stag}}(\beta)$ . Also, in staging PIMC, one must have the freedom to adjust the number of staging beads in order to maintain a reasonable acceptance rate, for instance 50%. The  $j/2$  staging beads that we get upon decimation may not give us the acceptance rate we require. We need to be able to readjust, if necessary, the number of staging beads (to  $j_{\text{new}}$ , say) such that the target acceptance ratio can be sustained, i.e. we would like to have  $n_{\text{new}} j_{\text{new}} = P/2$  rather than restricting ourselves to  $nj/2 = P/2$ . The following derivation will also address this issue. In what follows,  $\epsilon = \beta/P$ ,  $P' = P/2$ ,  $j' = j/2$ , and  $\epsilon' = \beta/P'$ , such that  $\omega_{P'}^2 = (\beta \hbar)^{-2} P' = \omega_P^2 / 2$  and  $\omega_{j'}^2 = (\beta \hbar)^{-2} (P'/j') = \omega_j^2$ . We now proceed by transforming the coordinates of the staging and end-point Trotter beads as follows:

$$\mathbf{u}'_{i,sj'+k'} = \sqrt{\frac{2k'-1}{k'}} \mathbf{u}_{i,sj'+k'}, \quad (7)$$

$$\mathbf{u}'_{i,sj'+1} = \mathbf{u}_{i,sj'+1}. \quad (8)$$

The Jacobian for the above coordinate transformation gives:

$$\overbrace{d\mathbf{u}_{1,1} \cdots d\mathbf{u}_{i,t} \cdots d\mathbf{u}_{N,P}}^{t \text{ odd only}} = \prod_{k'=2}^{j'} \left( \frac{k'}{2k'-1} \right)^{3Nn/2} d\mathbf{u}'_{1,1} \cdots d\mathbf{u}'_{i,t} \cdots d\mathbf{u}'_{N,P/2} \quad (9)$$

Upon carrying out the change of coordinates and the associated renumbering of indices,

we get

$$\begin{aligned}
Q_{P/2}^{\text{stag}}(\beta) &= \left\{ \frac{\beta m \omega_j^2}{2\pi} \prod_{\substack{k=2 \\ k \text{ odd only}}}^j \left( \frac{\beta \alpha_k}{\pi} \right) \prod_{k'=2}^{j'} \left( \frac{k'}{2k'-1} \right) \right\}^{3Nn/2} \\
&\times \int d\mathbf{u}'_{1,1} \cdots d\mathbf{u}'_{i,t} \cdots d\mathbf{u}'_{N,P'} \\
&\times \exp \left[ - \sum_{i=1}^N \sum_{s=0}^{n-1} \frac{m}{2j'\epsilon'\hbar^2} |\mathbf{u}'_{i,sj'+1} - \mathbf{u}'_{i,(s+1)j'+1}|^2 \right] \\
&\times \exp \left[ - \sum_{i=1}^N \sum_{s=0}^{n-1} \sum_{k'=2}^{j'} \frac{\beta}{2} m_{k'} \omega_{P'}^2 \mathbf{u}'_{i,sj'+k'}{}^2 \right] \\
&\times \exp \left[ - \frac{\beta}{P'} \sum_{t=1}^{P'} V_{\text{cl}}(\{\mathbf{r}_i(\mathbf{u}')\}; t) \right]. \tag{10}
\end{aligned}$$

Consider the following identity [28, 29, 33] for PIMC, generalized to 3 dimensions here. This identity is written for the first staging segment of the  $i$ -th quantum particle's polymer chain, but it holds true for any staging segment:

$$\begin{aligned}
\rho_0(\mathbf{x}_{i,1}, \mathbf{x}_{i,2}; \epsilon) \cdots \rho_0(\mathbf{x}_{i,j}, \mathbf{x}_{i,j+1}; \epsilon) &= \prod_{k=2}^j \left( \frac{\beta \alpha_k}{\pi} \right)^{3/2} \exp \left[ - \beta \alpha_k \mathbf{u}'_{i,k}{}^2 \right] \\
&\times \left( \frac{m}{2\pi\hbar^2 j \epsilon} \right)^{3/2} \exp \left[ - \frac{m}{2j\epsilon\hbar^2} |\mathbf{u}'_{i,1} - \mathbf{u}'_{i,j+1}|^2 \right], \tag{11}
\end{aligned}$$

where

$$\rho_0(\mathbf{x}_{i,t}, \mathbf{x}_{i,t+1}; \epsilon) = \left( \frac{m}{2\pi\hbar^2 \epsilon} \right)^{3/2} \exp \left[ - \frac{m}{2\hbar^2 \epsilon} |\mathbf{x}_{i,t} - \mathbf{x}_{i,t+1}|^2 \right]. \tag{12}$$

In the above equations,  $\{\mathbf{x}_{i,t}\}$  and  $\{\mathbf{u}'_{i,t}\}$  are related as follows:

$$\mathbf{u}'_{i,k} = \mathbf{x}_{i,k} - \mathbf{x}_{i,k}^*, \quad \text{for } k = 2, \dots, j \tag{13}$$

$$\mathbf{u}'_{i,k} = \mathbf{x}_{i,k}, \quad \text{for } k = 1 \text{ or } j + 1 \tag{14}$$

where

$$\mathbf{x}_{i,k}^* = \frac{(k-1)\mathbf{x}_{i,k+1} + \mathbf{x}_{i,1}}{k}. \tag{15}$$

We now express the integrand of  $Q_{P/2}^{\text{stag}}(\beta)$  as a product of factors, each of which has the same form as Eq. (11). This is done by introducing appropriate prefactors and regrouping the exponential factors involving end-point and staging beads. After some

tedious but straight-forward algebra, we get the following simple expression:

$$\begin{aligned}
 Q_{P/2}^{\text{stag}}(\beta) &= \int d\mathbf{u}'_{1,1} \cdots d\mathbf{u}'_{i,t} \cdots d\mathbf{u}'_{N,P'} \\
 &\times \left[ \prod_{i=1}^N \prod_{s=0}^{n-1} \underbrace{\rho_0(\mathbf{x}_{i,sj'+1}, \mathbf{x}_{i,sj'+2}; \epsilon') \cdots \rho_0(\mathbf{x}_{i,(s+1)j'}, \mathbf{x}_{i,(s+1)j'+1}; \epsilon')}_{j' \text{ factors of } \rho_0 \text{'s}} \right] \\
 &\times \exp \left[ -\frac{\beta}{P'} \sum_{t=1}^{P'} V_{\text{cl}}(\{\mathbf{r}_i(\mathbf{u}')\}; t) \right]. \tag{16}
 \end{aligned}$$

There are  $n$  segments, each consisting of  $j'$  factors of  $\rho_0$ 's. Therefore the total number of  $\rho_0$  factors is  $nj' = nj/2 = P/2$ . We are free to group  $j_{\text{new}}$  of these factors together such that  $n_{\text{new}}j_{\text{new}} = P/2$ . Then,

$$\begin{aligned}
 Q_{P/2}^{\text{stag}}(\beta) &= \int d\mathbf{u}'_{1,1} \cdots d\mathbf{u}'_{i,t} \cdots d\mathbf{u}'_{N,P'} \\
 &\times \left[ \prod_{i=1}^N \prod_{s=0}^{n_{\text{new}}-1} \underbrace{\rho_0(\mathbf{x}_{i,sj_{\text{new}}+1}, \mathbf{x}_{i,sj_{\text{new}}+2}; \epsilon') \cdots \rho_0(\mathbf{x}_{i,(s+1)j_{\text{new}}}, \mathbf{x}_{i,(s+1)j_{\text{new}}+1}; \epsilon')}_{j_{\text{new}} \text{ factors of } \rho_0 \text{'s}} \right] \\
 &\times \exp \left[ -\frac{\beta}{P'} \sum_{t=1}^{P'} V_{\text{cl}}(\{\mathbf{r}_i(\mathbf{u}')\}; t) \right]. \tag{17}
 \end{aligned}$$

Finally, using the identity in Eq. (11) in reverse, we obtain:

$$\begin{aligned}
 Q_{P'}^{\text{stag}}(\beta) &= \left\{ \left( \frac{\beta m \omega_{j_{\text{new}}}^2}{2\pi} \right) \prod_{k=2}^{j_{\text{new}}} \left( \frac{\beta m_k \omega_{P'}^2}{2\pi} \right) \right\}^{3Nn_{\text{new}}/2} \int d\mathbf{u}'_{1,1} \cdots d\mathbf{u}'_{i,t} \cdots d\mathbf{u}'_{N,P'} \\
 &\times \exp \left[ -\beta \left( \sum_{i=1}^N \sum_{s=0}^{n_{\text{new}}-1} \frac{m \omega_{j_{\text{new}}}^2}{2} |\mathbf{u}'_{i,sj_{\text{new}}+1} - \mathbf{u}'_{i,(s+1)j_{\text{new}}+1}|^2 \right. \right. \\
 &\quad \left. \left. + \sum_{i=1}^N \sum_{s=0}^{n_{\text{new}}-1} \sum_{k=2}^{j_{\text{new}}} \frac{m_k \omega_{P'}^2}{2} \mathbf{u}'_{i,sj_{\text{new}}+k} + \frac{1}{P'} \sum_{t=1}^{P'} V_{\text{cl}}(\{\mathbf{r}_i(\mathbf{u}')\}; t) \right) \right]. \tag{18}
 \end{aligned}$$

Hence, we have renormalized the staging Hamiltonian. It has exactly the same form as Eq. (2), but with only half the total number of degrees of freedom as before, since there are now  $P' = P/2$  instead of  $P$  Trotter beads. Clearly, the process can be repeated until one reaches the classical limit where  $P = 1$ , if so wished. In addition, we have also shown that upon renormalization, we are free to readjust the number of staging beads such that the target acceptance ratio can be maintained. This is important computationally for the efficient implementation of staging PIMC.

#### 4 Investigational Studies

The BLN protein model studied in this paper has the following potential energy:

$$\begin{aligned}
 V_{\text{cl}}(\{\mathbf{r}_i\}) = & \sum_{i=1}^{N-1} \frac{k_r}{2} (|\mathbf{r}_{i+1} - \mathbf{r}_i| - a)^2 + \sum_{i=1}^{N-2} \frac{k_\theta}{2} (\theta_i - \theta_0)^2 \\
 & + \sum_{i=1}^{N-3} [A_i(1 + \cos(\phi_i)) + B_i(1 + \cos(3\phi_i))] \\
 & + 4\epsilon \sum_{i=1}^{N-3} \sum_{j=i+3}^N C_{ij} \left[ \left( \frac{\sigma}{r_{ij}} \right)^{12} - D_{ij} \left( \frac{\sigma}{r_{ij}} \right)^6 \right],
 \end{aligned} \tag{19}$$

where

$$\begin{aligned}
 C_{ij} = 1, \quad D_{ij} = 1 & \quad \text{if } i, j \in B \\
 C_{ij} = \frac{2}{3}, \quad D_{ij} = -1 & \quad \text{if } i \in L, j \in B, L \\
 C_{ij} = 1, \quad D_{ij} = 0 & \quad \text{if } i \in N, j \in B, L, N.
 \end{aligned}$$

The letter codes B,L and N represent hydrophobic, hydrophilic and neutral protein residues, respectively. The sequence of the 46-residue model protein used in this study is  $B_9N_3(LB)_4N_3B_9N_3(LB)_5L$ . Reduced units are used throughout this article, unless otherwise stated. In addition, the mass of each residue  $m$ , Boltzmann constant  $k_B$ , the energy unit  $\epsilon$ , the Lennard-Jones parameter  $\sigma$ , and the bond length  $a$  are set to unity. In Eq. (19),  $k_r = 400\epsilon/a^2$ ,  $k_\theta = 20\epsilon/\text{rad}^2$ , and  $\theta_0 = 1.8326$  rad. For the dihedral-angle potential term, if two or more of the four defining residues of  $\phi_i$  are neutral (N), then  $A_i = 0, B_i = 0.2\epsilon$ , otherwise  $A_i = B_i = 1.2\epsilon$ . A weak boundary potential  $V_{\text{bp}}(\{\mathbf{r}_i\}) = \sum_{i=1}^N (k_b/2)(\mathbf{r}_i - \mathbf{r}_{\text{com}})^2$  is also utilized to prevent the protein from dissociation and also to encourage folding.

The procedure for the global optimization of the 46-residue protein with the QTAR algorithm will be described next. In our implementation, we control the annealing of  $\hbar$  through the parameter  $k_P \equiv m\omega_P^2$ : a decrease in the value of  $\hbar$  (for fixed  $P$ ) actually corresponds to an increase in the value of  $k_P$ .

1. Generate a random initial protein configuration.
2. Initialize the Trotter number  $P$  to  $P_0$ , the thermal temperature  $T$  to  $T_0$  and  $k_P$  to  $k_{P_0}$ . Quantize the classical configuration by going to step 3.
3. Perform  $n_{\text{staging}}$  staging PIMC passes with Eq. (2). If  $P$  gets relatively smaller (typically  $\leq 64$  here), perform  $n_{\text{local}}$  local and  $n_{\text{global}}$  global PIMC passes with Eq. (1) instead. After *each* PIMC pass,  $T$  is decreased linearly by  $\Delta T$ , and  $k_P$  is increased linearly by  $\Delta k_P$ .
4. Reduce  $P$  to  $P' = P/2$  by decimating out Trotter beads through renormalization. The number of PIMC passes for this new  $P'$ -stage is doubled such that the total number of MC sweeps in each  $P$ -stage remains constant. Now go back to step 3. This whole process is repeated until  $P = 1$ , when an *intermediate* classical configuration is obtained.

5. Halt if the stop criterion is met. Otherwise, repeat the quantum thermal annealing procedure with the intermediate classical configuration by going to step 2.

Steps 2–4 constitute a QTAR *cycle*. Twenty simulation trials, each with a different initial random configuration, are conducted with QTAR. The initial number of Trotter beads on each residue is set to be  $P_0 = 256$ . Staging PIMC moves are then performed for  $n_{\text{staging}} = 15$  passes, after which the renormalization operation is used to remove half the total number of Trotter beads from the system. The number of staging passes is then doubled to 30 for  $P = 128$ , as described by the procedure above. This scheme ensures that the amount of configuration space exploration at each quantum regime, as represented by  $P = P_0, P_0/2, \dots, 2, 1$ , is the same. For  $P \leq 64$ , local and global moves are used instead of staging moves. PIMC moves and renormalization are thus carried out sequentially in this manner until we reach  $P = 1$ , which is the classical regime. Within each QTAR cycle, the thermal temperature  $T$  is annealed linearly

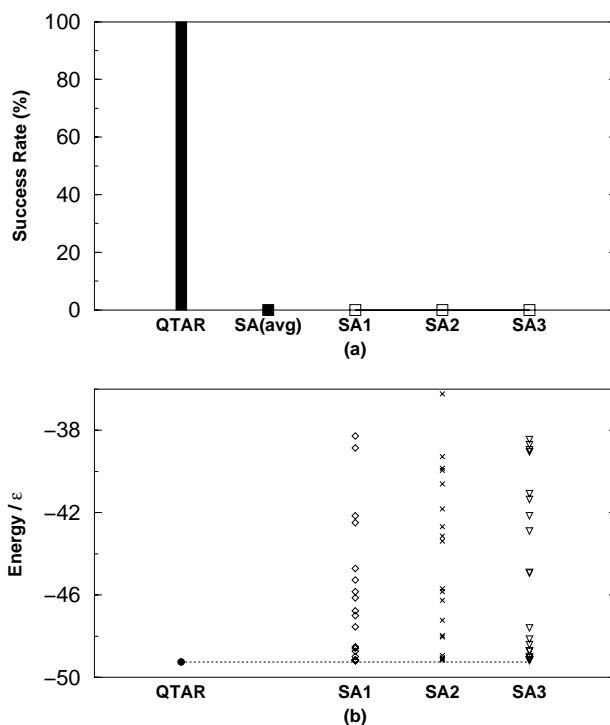


**Fig. 1** (a) QTAR is able to locate the global minimum of a frustrated 46-residue BLN model protein with a 100% success rate. Simulated annealing (SA), on the other hand, is unable to locate the global minimum even once, even though 3 separate annealing schedules (SA1 to SA3) are attempted. Each bar represents 20 independent simulation runs done using the same total amount of CPU time. SA(avg) represents the averaged results of SA1 to SA3. (b) The corresponding minimum energies attained with the forementioned QTAR and SA schedules. The global minimum of the 46-mer is represented by the dotted line.

from 0.2 to 0.02. At the end of each cycle, the intermediate classical configuration so obtained is subjected to a conjugate gradient refinement of its energy. This whole process is repeated until the currently known global minimum of the 46-mer is found.

For comparison purposes, we also conducted 3 independent sets of 20 simulated annealing (SA) runs using different annealing schedules on the same system. Each set of 20 runs utilizes the same total amount of CPU time as the set of 20 QTAR trials above. The results from the two methods are shown in Fig. 1. QTAR is able to locate the correct global minimum of the 46-mer without fail while SA is not able to do that even once. The presence of a large number of higher energy metastable states, in addition to the frustrated nature of the 46-mer, both contribute to the failure of SA in the global optimization of this system. QTAR, on the other hand, is able to overcome these problems effectively. A more detailed presentation and discussion of the simulation results can be found in Ref. [2].

## 5 Conclusions

In this paper, we present the details of our renormalization approach for global optimization with quantum thermal annealing. In particular, the renormalization of the staging Hamiltonian used in PIMC is carried out in detail to establish the mathematical basis behind our method. A comparison study on a highly frustrated system, a 46-residue BLN model protein, illustrates the effectiveness and efficiency of QTAR over an established and widely used method like simulated annealing.

This work was funded by the National Institutes of Health under Grants GM43340 and RR-06892. One of us (B.J.B.) would like to acknowledge many provocative scientific discussions with Peter Hänggi who is still young enough to appreciate and to contribute great science.

## References

- [1] Y. H. Lee and B. J. Berne, *J. Phys. Chem. A* **104** (2000) 86
- [2] Y. H. Lee and B. J. Berne, *J. Phys. Chem. A*, in press (2000)
- [3] S. Kirkpatrick, C. D. Gelatt Jr., and M. P. Vecchi, *Science* **220** (1983) 671
- [4] F. H. Stillinger, *Phys. Rev. B* **32** (1985) 3134
- [5] E. O. Purisima and H. A. Scheraga, *Proc. Natl. Acad. Sci. USA* **83** (1986) 2782
- [6] Z. Li and H. A. Scheraga, *Proc. Natl. Acad. Sci. USA* **84** (1987) 15
- [7] Z. Li and H. A. Scheraga, *Proc. Natl. Acad. Sci. USA* **84** (1987) 6611
- [8] B. A. Berg and T. Neuhaus, *Phys. Lett. B* **267** (1991) 249
- [9] D. Shalloway, *Global Optimization* **2** (1992) 281
- [10] P. Amara, D. Hsu, and J. E. Straub, *J. Phys. Chem.* **97** (1993) 6715
- [11] T. C. Beutler and W. F. van Gunsteren, *J. Chem. Phys.* **101** (1994) 1417
- [12] J. D. Doll and D. L. Freeman, *IEEE Comput. Sci. Eng.* **1** (1994) 22
- [13] U. H. E. Hansmann and Y. Okamoto, *Physica A* **212** (1994) 415
- [14] J. Ma and J. E. Straub, *J. Chem. Phys.* **101** (1994) 533
- [15] D. J. Wales and J. P. K. Doye, *J. Phys. Chem. A* **101** (1997) 5111
- [16] T. Kadowaki and H. Nishimori, *Phys. Rev. E* **58** (1998) 5355
- [17] D. B. Faken, A. F. Voter, D. L. Freeman, and J. D. Doll, *J. Phys. Chem. A* **103** (1999) 9521
- [18] H. Xu and B. J. Berne, *J. Chem. Phys.* **112** (2000) 2701
- [19] G. Stolovitzky and B. J. Berne, submitted to *Proc. Natl. Acad. Sci. USA* (2000)
- [20] J. D. Honeycutt and D. Thirumalai, *Proc. Natl. Acad. Sci. USA* **87** (1990) 3526

- [21] H. Nymeyer, A. E. García, and J. N. Onuchic, Proc. Natl. Acad. Sci. USA **95** (1998) 5921
- [22] M. A. Miller and D. J. Wales, J. Chem. Phys. **111** (1999) 6610
- [23] R. P. Feynman and A. R. Hibbs, *Quantum mechanics and path integrals*, McGraw-Hill, New York 1965
- [24] H. F. Jordon and L. D. Fosdick, Phys. Rev. **171** (1968) 128
- [25] J. A. Barker, J. Chem. Phys. **70** (1979) 2914
- [26] B. J. Berne and D. Thirumalai, Ann. Rev. Phys. Chem. **37** (1986) 401
- [27] D. M. Ceperley, Rev. Mod. Phys. **67** (1995) 279
- [28] E. L. Pollock and D. M. Ceperley, Phys. Rev. B **30** (1984) 2555
- [29] M. E. Tuckerman, B. J. Berne, G. J. Martyna, and M. L. Klein, J. Chem. Phys. **99** (1993) 2796
- [30] A. A. Migdal, Sov. Phys. JETP **42** (1975) 413
- [31] A. A. Migdal, Sov. Phys. JETP **42** (1975) 743
- [32] L. P. Kadanoff, Ann. Phys. (N.Y.) **100** (1976) 359
- [33] M. Sprik, M. L. Klein, and D. Chandler, Phys. Rev. B **31** (1985) 4234